Surface Heat Budget of the Arctic Ocean

BY TANEIL UTTAL, JUDITH A. CURRY, MILES G. MCPHEE, DONALD K. PEROVICH, RICHARD E. MORITZ, JAMES A. MASLANIK, PETER S. GUEST, HARRY L. STERN, JAMES A. MOORE, RENE TURENNE, ANDREAS HEIBERG, MARK. C. SERREZE, DONALD P. WYLIE, OLA G. PERSSON, CLAYTON A. PAULSON, CHRISTOPHER HALLE, JAMES H. MORISON, PATRICIA A. WHEELER, ALEXANDER MAKSHTAS, HAROLD WELCH, MATTHEW D. SHUPE, JANET M. INTRIERI, KNUT STAMNES, RONALD W. LINDSEY, ROBERT PINKEL, W. SCOTT PEGAU, TIMOTHY P. STANTON, AND THOMAS C. GRENFELD

A year/long ice camp centered around a Canadian icebreaker frozen in the arctic ice pack successfully collected a wealth of atmospheric, oceanographic, and cryospheric data.

The Surface Heat Budget of the Arctic Ocean (SHEBA) is a research program designed to document, understand, and predict the physical processes that determine the surface energy budget and the sea–ice mass balance in the Arctic (Moritz et al. 1993; Perovich et al. 1999). The central motivation behind SHEBA lies in the fact that the Arctic has recently undergone significant changes that are hypothesized to be a combination of poorly understood natural modes of variability and anthropogenic greenhouse warming. In addition, general circulation models (GCMs) have large discrepancies in predictions of present and future climate in the Arctic (e.g., Randall et al. 1998), and consequently, large uncertainties about the how the Arctic influences global climate change. These difficulties are due, in large part, to an incomplete understanding of the physics of the vertical and horizontal energy exchanges within the ocean–ice–atmosphere system. The SHEBA program is based on the premise that improved understanding of physical processes is needed, and that such understanding must be based on detailed empirical observations. The stated objectives of SHEBA are the following:

AFFILIATIONS: UTTAL AND INTRIERI—NOAA/Environmental Technology Laboratory, Boulder, Colorado; CURRY AND MASLANIK—University of Colorado, Boulder, Colorado; MCPHEE—McPhee Research Company, Naches, Washington; PEROVICH AND GRENFELD—Cold Regions Research and Engineering Laboratory, U.S. Army, Hanover, New Hampshire; MORITZ, STERN, HEIBERG, MORISON, AND LINDSEY—University of Washington, Seattle, Washington; GUEST AND STANTON—Naval Postgraduate School, Monterey, California; MOORE—University Corporation for Atmospheric Research, Boulder, Colorado; TURENNE—Canadian Coast Guard, Quebec City, Quebec, Canada; SERREZE AND PERSSON—Cooperative Institute for Research in the Environmental Sciences, Boulder, Colorado; WYLIE—University of Wisconsin—Madison, Madison, Wisconsin; PAULSON, WHEELER, AND PEGAU—Oregon State University, Corvallis, Oregon; HALLE AND PINKEL—Scripps Institute of Oceanography, La Jolla, California; MAKSHTAS—University of Alaska, Fairbanks, Alaska; WELCH—Winnepeg, Canada; SHUPE—Science and Technology Corporation, Boulder, Colorado; STAMNES—Stevens Institute of Technology, Maplewood, New Jersey

CORRESPONDING AUTHOR: Taneil Uttal, NOAA/Environmental Technology Laboratory, R/E/ET6, 325 Broadway, Boulder, CO 80305-3328
E-mail: taneil.uttal@noaa.gov

In final form 13 September 2001

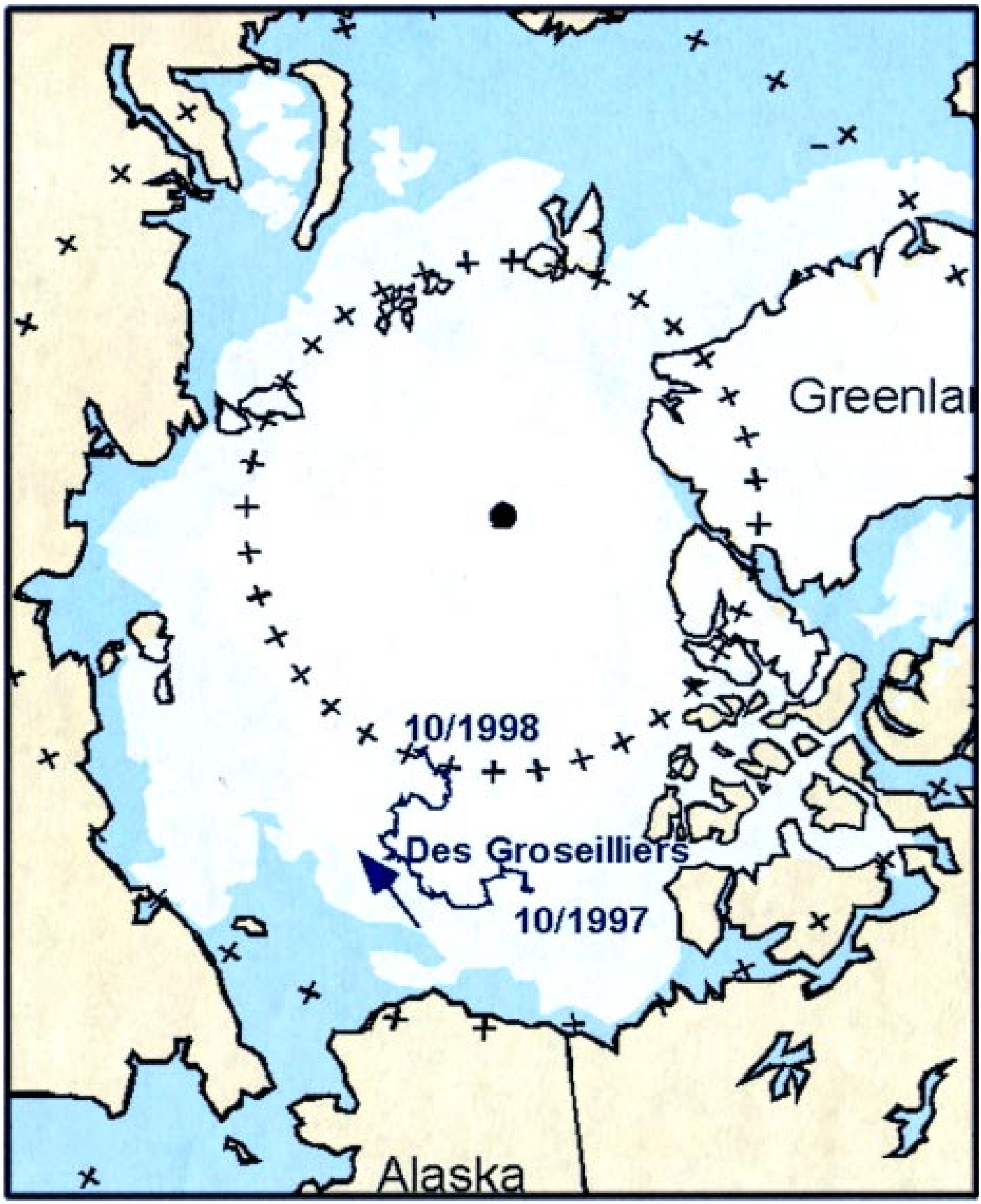

FIG. 6. The yearlong SHEBA drift. Blue zigzag line extending from Oct 1997 to Oct 1998.

Table 1. Annual cycle measurements.

Instrument	Collection start date	Collection end date	Data product
Deep ocean SeaCat CTD	12 Oct 1997	21 Sep 1998	Ocean depth, temperature, salinity, conductivity, density
Doppler sonar	26 Nov 1997	2 Oct 1998	Upper-ocean current
YoYo CTD (Seabird 911+)	11 Oct 1997	1 Oct 1998	Ocean temperature, conductivity, salinity, density
Dual-thermistor thermal	7 Oct 1997	22 Sep 1998	Thermal microstructure dissipation rate dissipation package
Turbulence mast	9 Oct 1997	26 Sep 1998	Ocean current speed/direction, temperature, salinity, salinity flux, turbulent heat flux, Reynolds stress
ARGOS drifter buoys (microCAT)	2 Oct 1997	2 Oct 1998	Conductivity, salinity, temperature, position
Buoys (thermistors)	14 Oct 1997	10 Feb 1998	Air and snow temperature, position
Buoys (thermistors)	26 Oct 1997	1 Oct 1998	Ice thickness
Snow gauges	11 Oct 1997	1 Oct 1998	Snow depth
Thermistors	13 Oct 1997	1 Oct 1998	Snow and ice temperature
Stress meters			Ice stress
GPS	1 Oct 1997	11 Oct 1998	Ice camp position and heading
Surface weather reports	29 Oct 1997	9 Oct 1998	Cloud-base height, visibility, cloud fraction, wind speed and direction, air temperature, dewpoint, pressure, pressure tendency, weather conditions
Nipher-shielded snow gauge	29 Oct 1997	9 Oct 1998	Liquid water equivalent precipitation
Optical rain gauge	1 Oct 1997		Precipitation rate
Portable Mesonet (PAM) stations	1 Nov 1997	1 Oct 1998	Pressure, temperature, relative humidity, wind speed and direction, broadband shortwave and longwave fluxes up and down
Scintillometer	20 Oct 1997	2 Aug 1998	Refractive index structure, inner scale of turbulence
10-m towers (thermometers, prop anemometers)	9 Oct 1997	1 Oct 1998	Temperature, dewpoint, wind speed and direction at 2 and 10 m, pressure
20-m tower (thermometers, anemometer)	1 Oct 1997	1 Oct 1998	Temperature, relative humidity, wind speed sonic and direction, friction velocity, sensible heat flux, surface and snow/ice temperature
Eppley radiometers	1 Oct 1997	1 Oct 1998	Broadband shortwave and longwave fluxes, down and up
35-GHz cloud radar	20 Oct 1997	1 Oct 1998	Radar reflectivities, Doppler velocities and spectral widths
523-nm depolarization lidar	1 Nov 1997	8 Aug 1998	Lidar backscatter, depolarization ratios
GLAS (Vaisala) rawinsonde	16 Oct 1997	15 Oct 1998	Pressure, temperature, relative humidity, wind speed and direction, position

Table 2. Seasonal measurements.

Instrument	Collection start date	Collection end date	Data product
Seabird SBE-25 CTD	10 Jun 1998	4 Aug 1998	Temperature, pressure, salinity, conductivity down to 60 m in leads
Seabird SBE-19 CTD	6 Jun 1998	9 Aug 1998	Temperature, pressure, salinity, conductivity at lead surface and down to 15 m in leads
AC-9	17 Jun 1998	4 Aug 1998	Optical properties, beam attenuation, absorption coefficient in leads
Eppley radiometer	7 Jun 1998	1 Aug 1998	Lead albedo
Buckets/filters	8 Oct 1997	4 Oct 1998	Beryllium-7 concentration
Mobile radiometric platform (IR thermometer, thermistor, pyranometers)	5 Apr 1998	8 May 1998	Air and snow temperature, albedo, flux—over ice, snow, and lead surfaces
Electromagnetic induction EM-31	2 Oct 1997	10 Oct 1998	Ice thickness distribution estimates
0.4-μm nucleopore filters	9 Apr 1998	14 Jul 1998	Soot content in snow and ice
Spectron engineering SF-590	11 Jun 1998	3 Sep 1998	Spectral albedo (300–2500 nm)
Zipp and zonen radiometer	1 Apr 1998	27 Sep 1998	Wavelength-integrated albedo
Magneprobe radar	25 Mar 1998	11 May 1998	Spatial (not temporal) snow cover
Geokon vibrating wire stress meters	1 Jun 1998	31 Aug1998	Ice stresses
Helicopter aerial photography	17 May 1998	4 Oct 1998	Photos of surface in 250 frames/flight: 5/17, 5/20, 6/10, 6/15, 6/22, 6/30, 7/08, 7/15, 7/20, 7/25, 8/7, 8/22, 9/11, 10/4
Helicopter IR photometry	10 Jun 1998	29 Aug 1998	IR photometry
Twin otter surface property survey	14 Oct 1997	11 May 1998	Surface temperatures and video
Tethered balloon (Vaisala T/RH/ wind sensors)	4 Dec 1997	19 July 1998	Pressure, temperature, relative humidity, wind speed and direction
Tethered balloon (cloud particle videometer)	5 May 1998	12 Oct 1998	Cloud particle sizes and concentrations
Tethered balloon (radiometer)	14 Sep 1998	21 Sep 1998	Hemispheric radiation

the Northwest Passage was not navigated until 1905. The beginning of scientific field experiments in the modern sense, with a primary emphasis on measuring physical properties of the arctic environment, can probably be assigned to the year 1937 when the Russians established a drifting ice camp composed of fur-lined tents. This camp, designated North Pole 1, was the first in a series of 31 long-term, research ice camps, which where consecutively designated NP1 to NP31. The NP camps were typically deployed by icebreaker

Table 3. Measurements made by collaborating programs

Instrument	Collection start date	Collection end date	Data product
SCICEX submarine	28 Sep 1997	1 Oct 1997	Ice thickness distribution, sonar ice drift profiles
Buoys	1 Oct 1997	1 Oct 1998	CTD data, mooring data
IOEB buoys (thermistors, R. M. Young probes, etc.)	30 Sep 1997	1 Oct 1998	Pressure, temperature, winds speed and direction, ice temperature profiles, biogeochemical data, position
IOEB buoys (CTD, ADCP)	30 Sep 1997	1 Oct 1998	Ocean temperature, salinity, ocean current profiles
Radiometers	1 Nov 1997	30 Sep 1998	Upwelling radiation and downwelling radiation
SkyRad (radiometers)	1 Nov 1997	30 Sep 1998	Downwelling radiation
Atmospheric emitted radiance interferometer (AERI)	25 Oct 1997	1 Jul 1998	Downwelling spectral radiances
Multifilter rotating shadowband radiometer	25 Oct 1997	30 Sep 1998	Downweling irradiances
Whole sky imager	25 Oct 1997		Visual images of atmospheric conditions
Microwave radiometer	25 Oct 1997	9 Sep 1998	Brightness temperatures at 23.8 and 31.4 GHz, integrated liquid water path, integrated water vapor path
Laser ceilometer	25 Oct 1997	30 Sep 1998	Cloud-base heights
Standard filter ozonemeter			Ozone concentrations
NASA Polar Pathfinder APP products (AVHRR)	1 Nov 1997	31 Oct 1998	Brightness temperature, surface temperature, radiance, albedo, solar zenith angle, surface type
Satellite (NOAA polar orbiter–AVHRR)	16 Sep 1997	1 Oct 1998	IR composite image
Satellite (SAR)	1 Nov 1997	8 Oct 1998	Ice motion and deformation
Satellite (SAR)	1 May 1998	15 Oct 1998	Floe size distribution
Satellite (RADARSAT)	1 Nov 1997	31 Oct 1998	Ice motion products
Satellite (RADARSAT)	1 Nov 1997	8 Oct 1998	Images and derived products

and supported by aircraft, and the standard tour of duty for the hardy inhabitants of these ice camps was 1 yr; the efforts of these Russian scientists resulted in a 54-yr-long record of measurements (Kahl et al. 1999). The U.S. drifting ice camp program started with the manning of ice island T3 in early 1950. Since then there have been over 50 ice camps deployed in various regions of the Arctic; most have been short-term, air-deployed, springtime operations when the combination of sunlight and sea-ice conditions optimized the environment for temporary human habitation.

Ships frozen into the ice have also been deployed for research with mixed results. In 1892 the *Fram,* under the leadership of Fridtjof Nansen, made a successful 3-yr drift across the polar basin collecting a wealth of scientific data. In the first part of this cen-

FIG. 1. The SHEBA ice camp in Oct 1997 immediately after setup. (Photo credit: Don Perovich.)

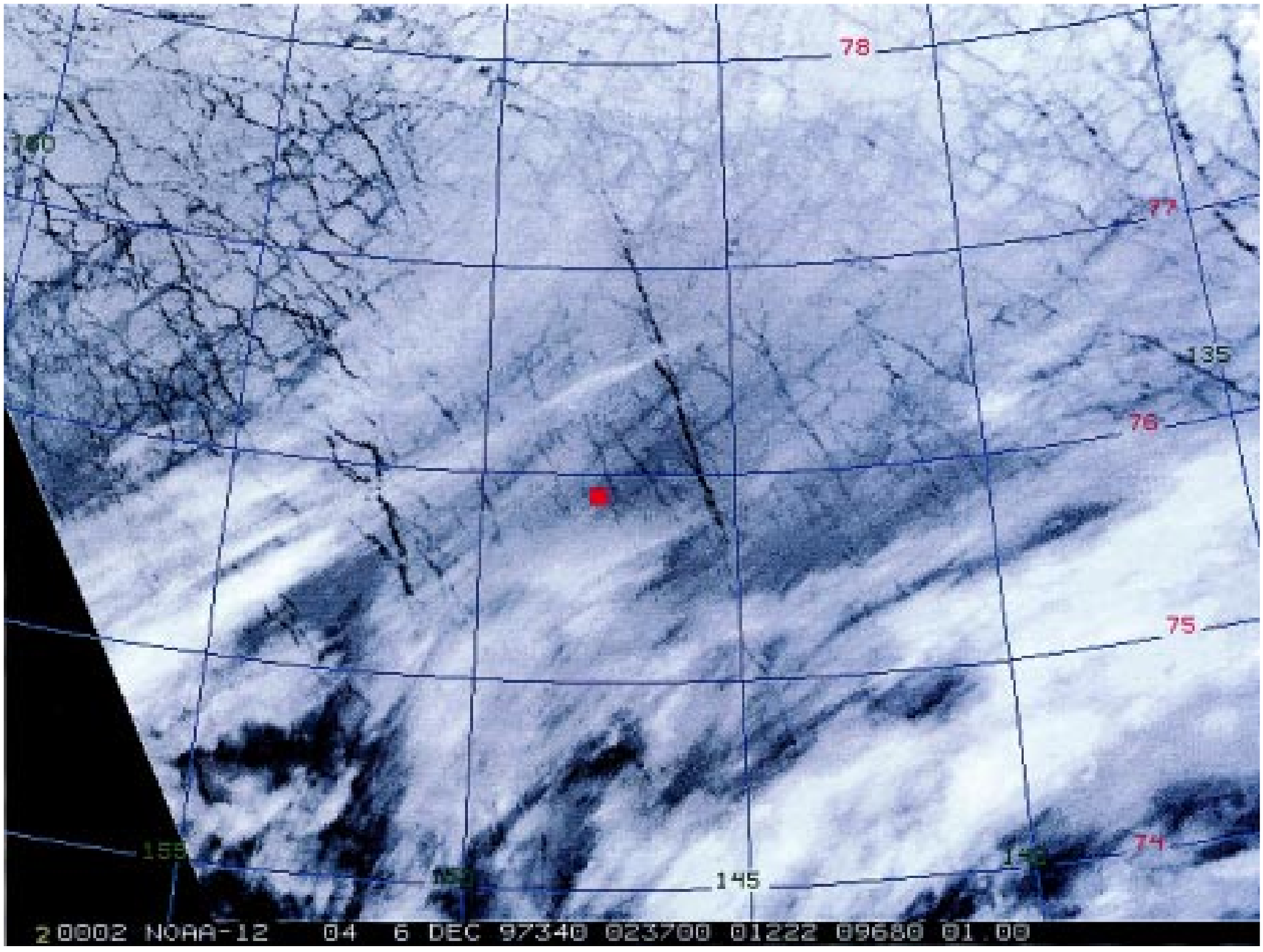

FIG. 2. Satellite image (0237 UTC 6 Dec) indicating elongated clouds over the ice camp (red square) that thicken to the south and clear to the north. The patterns in the ice are presumed to be old lead fractures that have frozen. The SHEBA ice camp is at 75°53′N and 148°15′W.

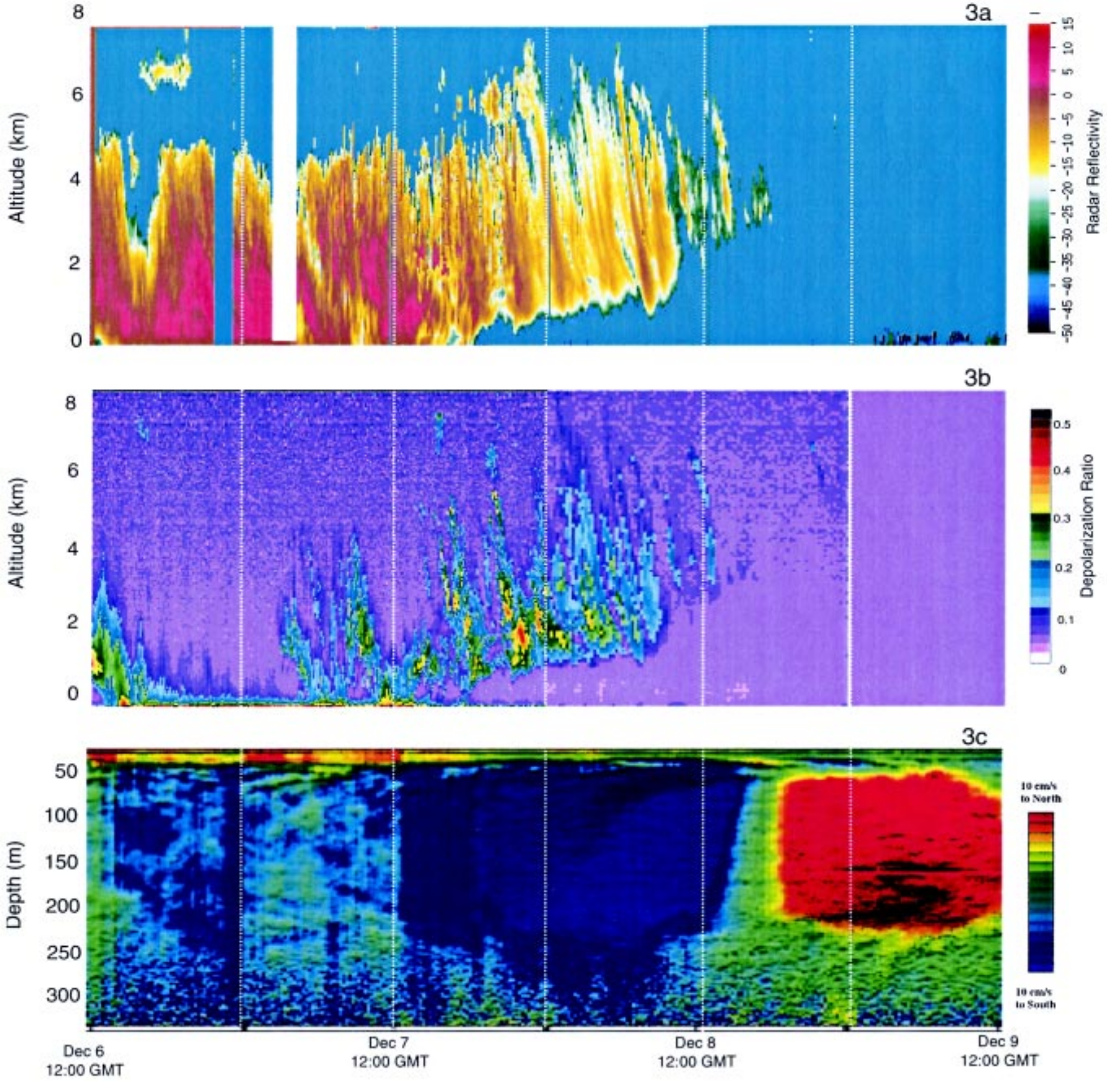

FIG. 3. Time–altitude/depth cross section of (a) radar reflectivity, (b) lidar depolarization, and (c) Doppler sonar ocean currents from 1200 UTC 6 Dec to 1200 UTC 9 Dec.

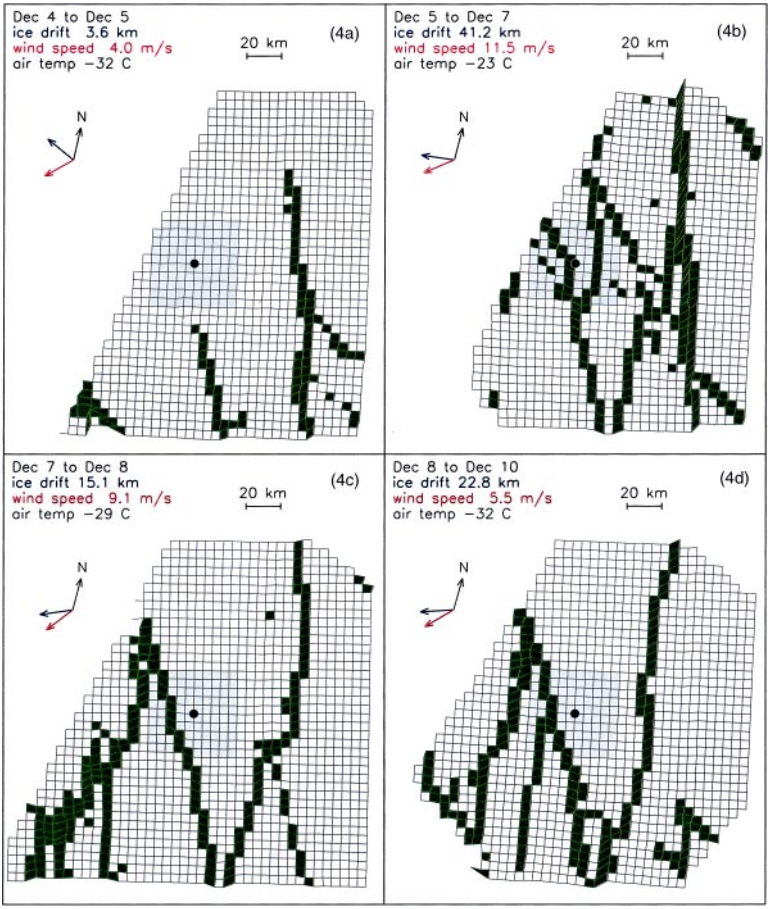

FIG. 4. Sea-ice deformation near the SHEBA ice camp from 4 to 10 Dec 1997. The ship is located at the black dot in the center of each panel. Green (deforming) cells show the pattern of active leads. These are derived from successive Radarsat SAR images from RGPS.

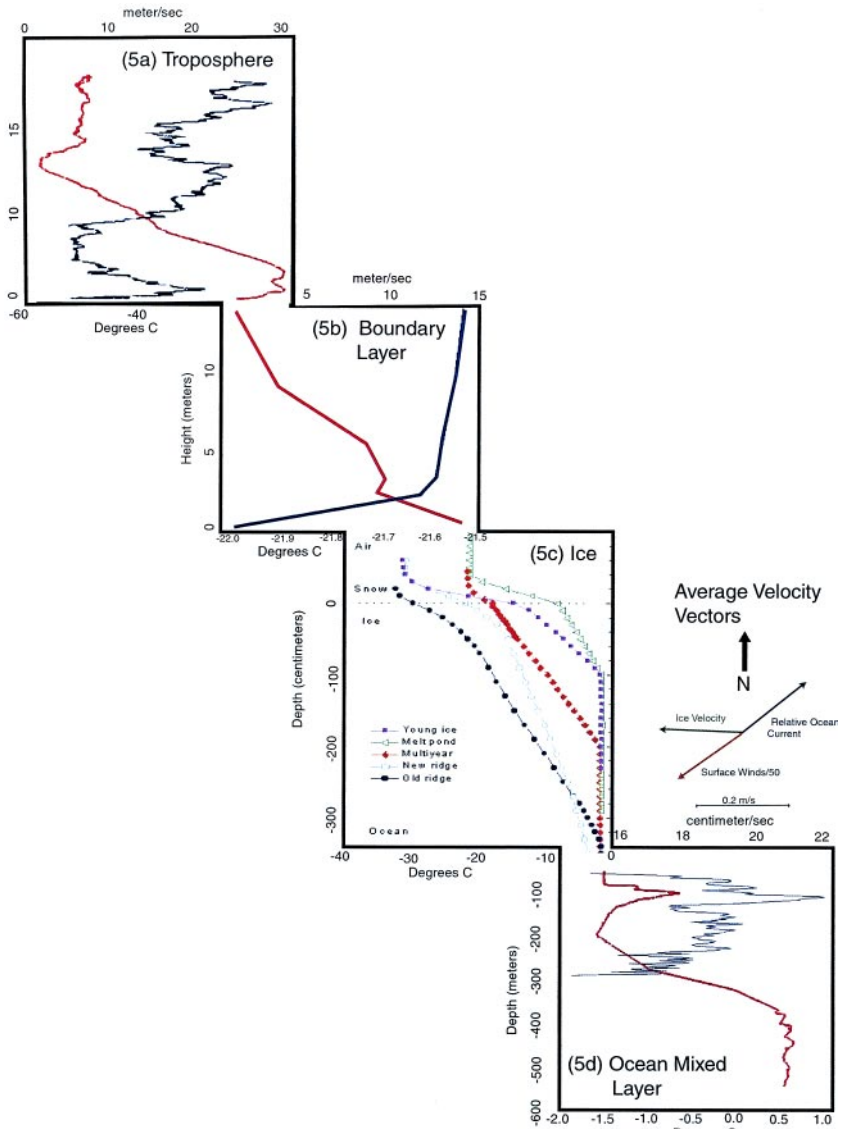

FIG. 5. Temperature and velocity profiles through the SHEBA column on 7 Dec 1997. (a) Rawinsonde temperature (red) and wind speed (blue), (b) 20-m meteorological tower temperature (red) and wind speed (blue), (c) ice thermistor temperature at a variety of sites, and (d) ocean CTD temperature (red) and Doppler velocity current speed (blue). Relative velocity vectors for surface wind, ice drift, and ocean current are shown to the right of (c).

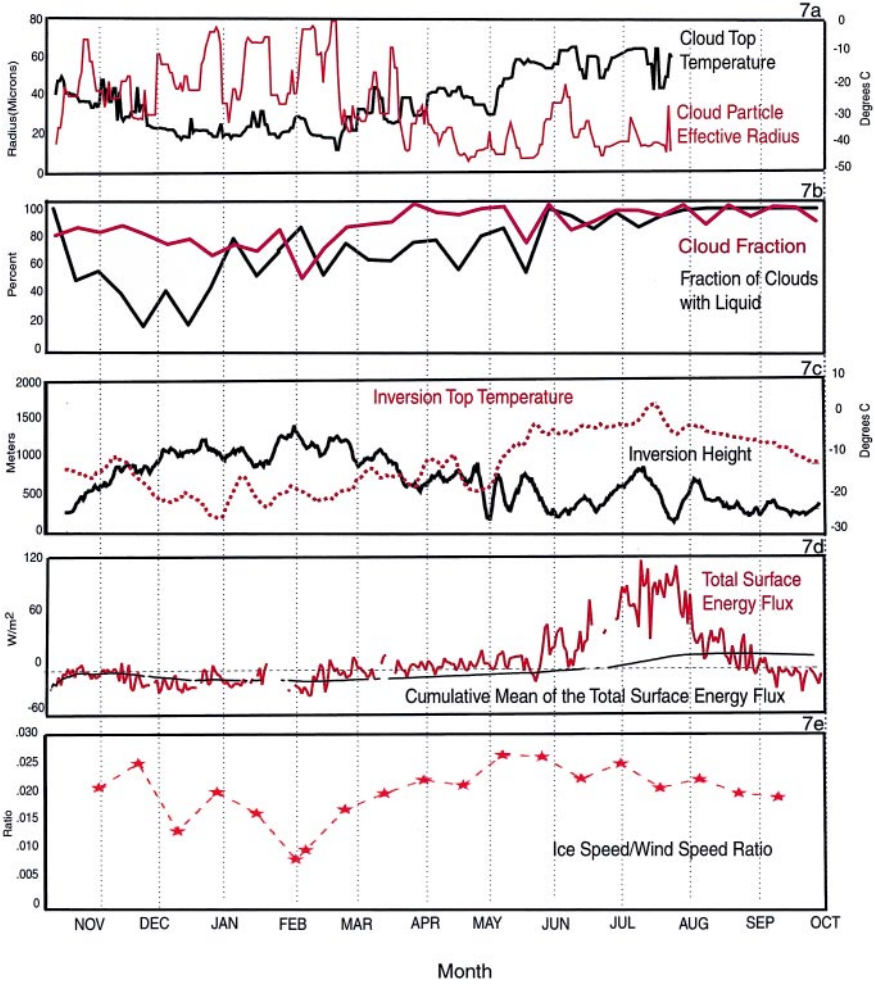

FIG. 7. Yearlong time series (a) cloud-top temperature and mean cloud particle radius from AVHRR Polar Pathfinder, (b) cloud fraction (percent) from 35-GHz cloud radar/depolarization lidar and percent of clouds with liquid water layers, (c) inversion top temperature and inversion top height from rawinsonde, (d) total net surface energy flux and cumulative mean of the total net surface energy flux from the 20-m tower, and (e) ratio of ice speed to wind speed.

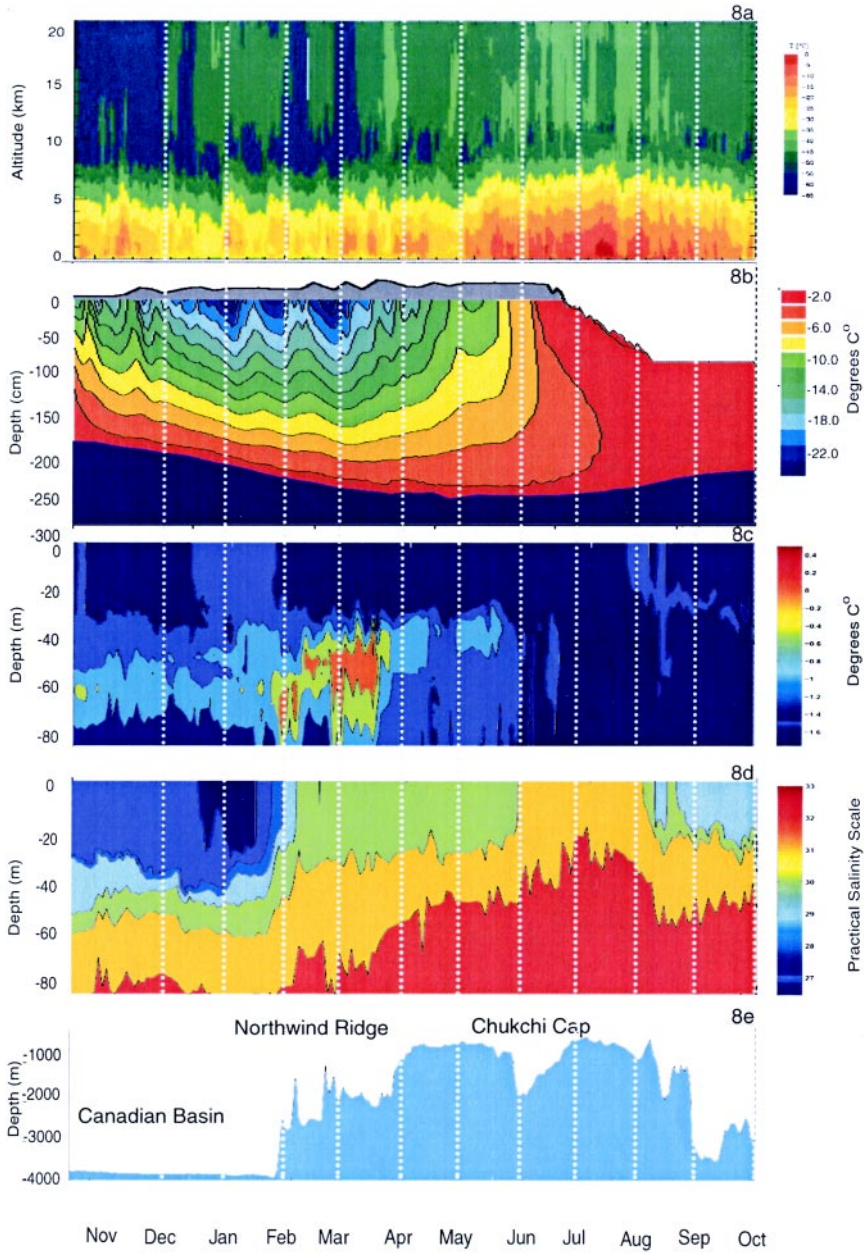

FIG. 8. Yearlong series of vertically resolved measurements: (a) rawinsonde temperatures, (b) ice temperatures and thickness with snow depth in gray (same cm scale), (c) ocean CTD temperature, (d) ocean CTD salinity, and (e) bathymetry.

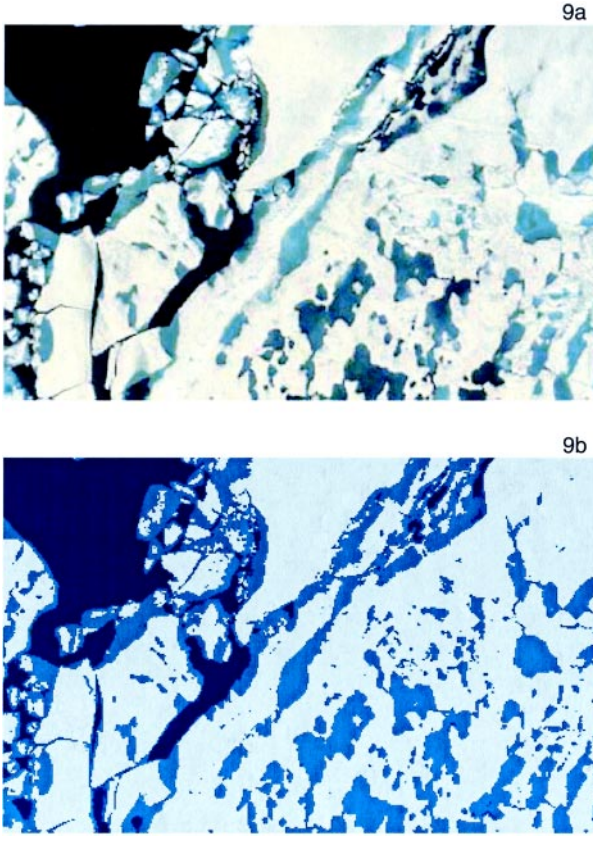

FIG. 9. (a) Aerial photography with 35-mm camera from helicopter; (b) classification of leads and open water (dark blue), meltponds (light blue), and ice (white) from digitized photo shown in (a).

more than four weeks. Very low salinity and temperatures well above freezing characterized the freshwater layer (Fig. 12). The strong vertical stratification associated with the freshwater layer inhibited mixing until late July for the upper 15 m of the ocean, and until early August for the ocean mixed layer.

Biologists measured a wide variety of parameters, primarily from a winch stationed on the ice, with casts between the surface and the ocean floor (sometimes as deep as 4 km) throughout the year. Some of the primary variables were measurements of oxygen, phosphorus, nitrogen, silica, bacterial activity, and respiration rates of the total zooplankton community throughout the water column. Biological laboratories were distributed in three seatainers on the ice as well as on the ship; these facilitated year-round work experiments on plankton, radioisotopes, pollutants, and other variables. Changes in oxygen and nutrients, bacterial activity, and respiration rate of the total zooplankton community showed that the productivity of the Arctic Ocean at the SHEBA ice station was much higher than expected. It is possible that this may be the result of a thinning ice cover and more extensive leads, resulting in increased available solar radiation for production. An example of relative snow cover and surface chlorophyll (μg/liter in the 0–50 m layer) between 29 April and 24 June is shown in Fig. 13 and an (unrelated) inset shows an example of an 8-mm copepod, the dominant zooplankton species.

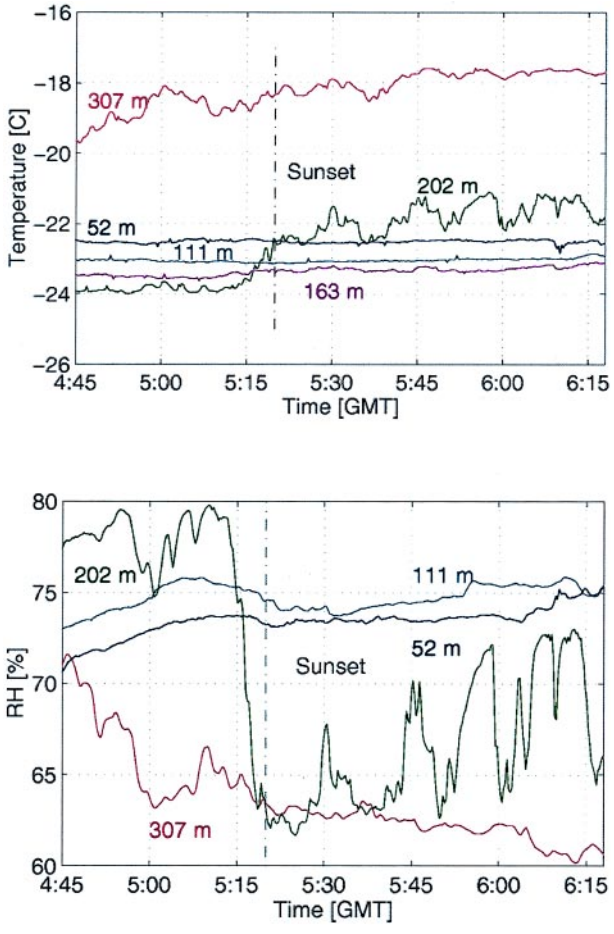

Fig. 11. Tethered balloon (top) temperatures at five levels, and (bottom) humidity at corresponding levels during sunset on 23 Mar 1998.

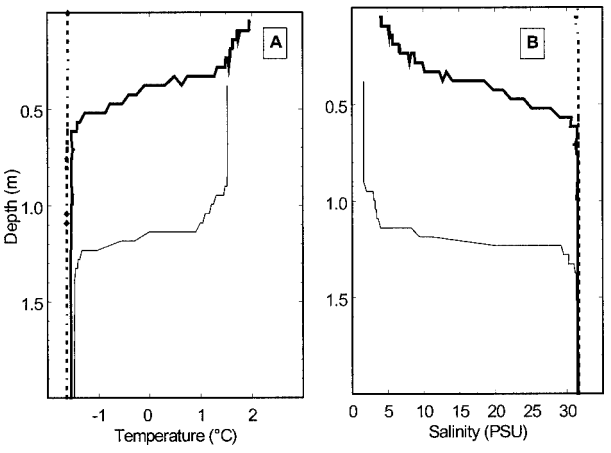

Fig. 12. Ocean CTD measurements in lead (a) temperature and (b) salinity. Profiles shown were collected on 19 Jun (dotted line), 11 Jul (thick line), and 22 Jul (thin line).

REPRESENTATIVENESS OF THE SHEBA YEAR. In light of the profound changes in the arctic environment that have occurred in the 1990s (Serreze et al. 2000), as well the fact that the SHEBA measurements will provide the baseline for a large number of process and model studies in coming years, it is important to assess how representative conditions were during SHEBA.

In the autumn of 1997 at the start of the SHEBA year, it was noted that the western Arctic appeared to be in an atypical state with an unusual lack of thick old ice. Recognizing that thin, first-year ice will melt earlier than old ice, McPhee et al. (1998) predicted a negative ice mass anomaly in the summer and autumn of 1998. This prediction proved to be accurate; 1998 was a record minimum in sea-ice extent in the western Arctic compared to historical records extending back to 1953 (Maslanik et al. 1999). During the summer of 1998, maximum seasonal distance between the ice edge and Point Barrow, Alaska (569 km), was 46% greater than the previous record year that occurred in the mid-1950s (390 km). Evidence indicates that negative sea-ice anomalies can be broadly understood in the context proposed by Rogers (1978) based on the composite analysis of summer-averaged sea level